The potential energy surface of excited singlet states of BCl by using the equation-of-motion coupled-cluster theory

ARTICLE *in* CHEMICAL PHYSICS LETTERS · MARCH 2001

Impact Factor: 1.9 · DOI: 10.1016/S0009-2614(01)00169-5

2 AUTHORS, INCLUDING:

Kyoung Koo Baeck
Gangneung-Wonju National University
44 PUBLICATIONS **424** CITATIONS

30 March 2001

ELSEVIER

Chemical Physics Letters 337 (2001) 190–198

CHEMICAL PHYSICS LETTERS

www.elsevier.nl/locate/cplett

The potential energy surface of excited singlet states of BCl by using the equation-of-motion coupled-cluster theory

Kyoung K. Baeck *, Youngdae Joo

Department of Chemistry, Kangnung National University, Kangnung, Kanwondo 210-702, South Korea

Received 15 August 2000; in final form 31 January 2001

Abstract

The excited singlet states of BCl are studied by using the equation-of-motion coupled-cluster singles and doubles theoretical method. The potential energy surfaces (PES) are constructed and the vibrational levels are calculated by using the Fourier-grid-Hamiltonian method. It is shown that $D\,^1\Sigma^+$ and $E\,^1\Sigma^+$ states correspond to the two stationary points of the same adiabatic PES with double minima. New high-lying four $^1\Sigma$, three $^1\Pi$, two $^1\Delta$, and one $^1\Phi$ excited state are tentatively assigned, and their spectroscopic constants are also derived. © 2001 Published by Elsevier Science B.V.

1. Introduction

The existence, and properties, of electronically excited states of BCl have been attracting much attention recently [1–3], partially because of its possible involvement in the radio frequency (RF) plasma etching with BCl_3 feed-gas. For a long time, however, the collection of spectroscopic and thermodynamic data on BCl has been limited to the ground singlet ($X\,^1\Sigma^+$), the lowest triplet ($a\,^3\Pi_1$), and the first excited singlet ($A\,^1\Pi$) states [4–9]. About five years ago, Verma had reported a new absorption spectra of BCl, and designated the four new states as $B\,^1\Sigma^+, C\,^1\Pi, D\,^1\Sigma^+$, and $E\,^1\Sigma^+$ [10]. According to this work, the difference between the v_{00} of the D and E states is just 307.6 cm^{-1}.

In a very recent study by using the resonance-enhanced multiphoton ionization (REMPI) experiment and the equation-of-motion coupled-cluster singles and doubles (EOM-CCSD) theoretical calculations, Irikura et al. have observed and defined a new singlet state [11], and they have shown that the new state is located at about 0.56 eV below the $B\,^1\Sigma^+$ state. The new state is named as $F\,^1\Sigma^+$. They also have characterized three new triplet states: $f\,^3\Sigma^+, b\,^3\Sigma^+$, and $c\,^3\Pi$. In addition to the theoretical interpretation of the F, B, and C singlet states, Irikura has provided enough information to resolve the controversy surrounding the ionization and dissociation energies of BCl. The theoretical information and interpretation of the D and E singlet states, however, are still lacking. Though the v_{00}'s and rotational constants of the D and E states are obtained in the spectroscopic work of Verma [10], the calculated values by Irikura et al. are far from sufficient to characterize or distinguish the two states.

* Corresponding author. Fax: +82-33-647-1183.

E-mail address: baeck@knusun.kangnung.ac.kr (K.K. Baeck).

0009-2614/01/$ - see front matter © 2001 Published by Elsevier Science B.V.
PII: S0009-2614(01)00169-5

This work was initiated to provide further theoretical information for the D and E states, and our study shows a new adiabatic potential energy surface (PES) connecting the two states, D and E. The information for the X, A, F, B, and C states of BCl are also supplied in this theoretical work to augment the previous experimental and theoretical studies [10,11]. In addition to these states, the present work provides spectroscopic constants of new additional high-lying four $^1\Sigma$, three $^1\Pi$, two $^1\Delta$, and one $^1\Phi$ excited states.

A brief description of our calculation methodology is given in the next section followed by the section presenting and discussing our results. One of our main emphases in this work is to provide the adiabatic PES of very high quality for the D and E singlet states as well as spectroscopic constants of other new high-lying singlet states.

2. Computation methods

The accuracy and reliability of the EOM-CCSD method [12] for excited singlet states have been discussed elsewhere [13], and the application on the excited states of BCl and BF in the previous work by Irikura et al. [11] has demonstrated its remarkable accuracy. We also applied the same EOM–CCSD method implemented in the ACES-II suit of programs [14]. Irikura et al. have employed the reasonably large aug-cc-pVTZ basis sets augmented with additional functions to accommodate Rydberg states. In order to support and augment their results, we made significantly larger and hugely exhaustive basis sets, (16s11p5d3f)/[9s9p5d3f] for B and (18s13p5d4f)/[8s8p5d4f] for Cl, by augmenting 2s2p1d and 1s1p type Rydberg functions to the Widmark–Malmqvist–Roos (WMR) basis sets [15] of B and Cl, respectively. The exponents suggested by Dunning and Hey are used for the Rydberg functions: $\varsigma_{B,s} = 0.019, 0.0047$, $\varsigma_{B,p} = 0.015, 0.0041$, $\varsigma_{B,d} = 0.015$, $\varsigma_{Cl,s} = 0.025$, $\varsigma_{Cl,p} = 0.020$ [16].

Owing to the tremendous size of our basis sets, among the eleven occupied MOs of BCl the six innermost core molecular orbitals (MOs) corresponding to 1s atomic orbital (AO) of B atom and 1s-, 2s-, and 2p- AOs of Cl atom are dropped in the post-HF calculation. While only the five active occupied MOs are included, all the 156 virtual MOs are included in the electron correlation by the coupled-cluster singles and doubles (CCSD) [17] and the EOM–CCSD calculations for excited states. Just by dropping the six core MOs, the computation times are reduced down to about one tenth of the calculation with all MOs. The previous works on the effects of the dropped MOs on bond lengths, excitation energies, and vibrational frequencies of ground [18] and excited states [19,20] have shown that the magnitudes of the effect are about 0.3 pm, 0.03 eV, and 3% of the calculated bond lengths, excitation energies, and harmonic frequencies, respectively. Similar magnitude of the effects is also expected in the results of this work.

The total energies of electronic excited states are calculated by using the EOM–CCSD method [12] on top of the CCSD method [17] for the ground state at arbitrarily selected internuclear distances around anticipated equilibrium distances of several electronic states. The selected internuclear distances can be seen in Fig. 2. The adiabatic potential energy surface (PES) of a state is obtained by connecting the calculated points with the help of the avoided crossing rule between electron states of the same symmetry. It might be worth mentioning that the identification of the symmetry of an excited state needs a little caution in this theoretical calculation. The actual calculations are performed by using the C_{2v} subgroup while the true symmetry group of BCl is $C_{\infty h}$, and the correlation of symmetry species are $\Sigma \rightarrow A_1$, $\Pi \rightarrow B_1 + B_2$, and $\Delta \rightarrow A_1 + A_2$. As a result, the true symmetry of an excited state of A_1 symmetry is not clear whether it corresponds to Σ or Δ. Our EOM–CCSD calculation produces some excited A_1 states having exactly the same energy of the corresponding A_2 excited states. When such A_1 states are selected, then the remaining excited A_1 states correspond to Σ states.

Based on the overall feature of a PES, an appropriate functional form, which will be discussed in the next section, is selected for the fitting of the PES. The vibrational levels on a PES are obtained by using the Fourier-grid Hamiltonian method [21], and the spectroscopic parameters of the states

are determined by using the PES and the calculated vibrational levels.

The EOM–CCSD calculation provides us the t_1 amplitudes of an excited state [12], corresponding to the C_1 coefficients of CI methods, which give information about the leading electron configuration of an excited state. By using the t_1 amplitude, the change in the electron excitation of each excited state along the internuclear distance will be mentioned in the following section, and the change will be discussed in connection with the shape of the adiabatic PES. Further details concerning a nonadiabatic coupling and/or internal conversion are beyond the scope of this work.

3. Results and discussion

Before discussing our calculated results, it is helpful to consider the possible state correlation between molecular states and atomic states, as shown in Fig. 1. Both the B and Cl atoms have the ^{2}P ground electronic state. The excitation energy of the first excited state of Cl atom, ^{4}P state, is 8.92 eV, which is larger than the first ionization potential (IP) of B atom, 8.29803 ± 0.00002 eV [22]. Several excited electronic states of B atom are located below the IP of B atom, and the excitation energies of the lowest three states ^{4}P, ^{2}S, and ^{2}D are 3.57, 4.96, and 5.93 eV, respectively [22]. Because the electronic affinity (EA) of Cl atom is 3.6135 ± 0.0010 eV [22], the dissociation limit to the ionic pair of B^+ and Cl^- lies 4.6845 eV above the dissociated pair of B and Cl atoms in their ground electronic state. These facts imply that the Rydberg functions for B atom may be more important than those for Cl atom, and that is why we augmented 2s2p1d and 1s1p type Rydberg functions of B and Cl, respectively, to the WMR basis sets.

According to Wigner and Witmer [23], the $B(^2P) + Cl(^2P)$ dissociation limit correlates with three Σ, two Π, and one Δ states of BCl of singlet and triplet spin multiplicities. Though the $B(^4P) + Cl(^2P)$ limit also correlates with the same six states of triplet and quintet multiplicities, they are not relevant in this work because our concern here is limited to singlet states. On the other hand,

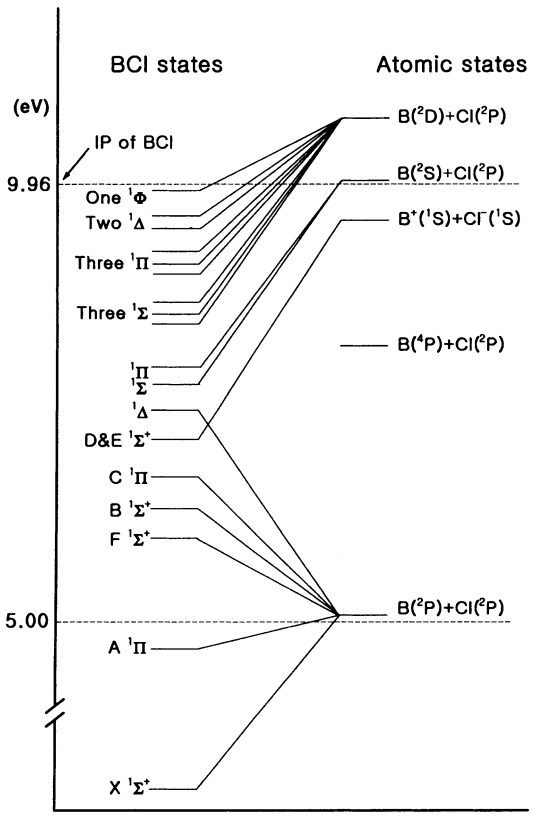

Fig. 1. The correlation diagram between electronic states.

the $B^+(^1S) + Cl^-(^1S)$ dissociation limit correlates to only one singlet Σ state. The $B(^2S) + Cl(^2P)$ limit correlates to one Σ and another Π state, while the $B(^2D) + Cl(^2P)$ limit correlates to three Σ, three Π, two Δ, and one Φ states of singlet and triplet multiplicities. The low-lying Σ states are designated here as Σ^+ according to Verma [10] and Irikura [11]. The dissociation energy and ionization energy of the ground state of BCl are 5.02 and 9.964 eV, respectively [11].

The combination of all these data suggests the possible correlation diagram as shown in Fig. 1, which can be compared with the actual PES of our calculation shown in Fig. 2. To provide a clearer picture, the PES of excited states obtained in the present calculations are divided into three figures according to their symmetry; Fig. 2a–c illustrate the singlet states of Σ, Π, and other (Δ and Φ) symmetry, respectively.

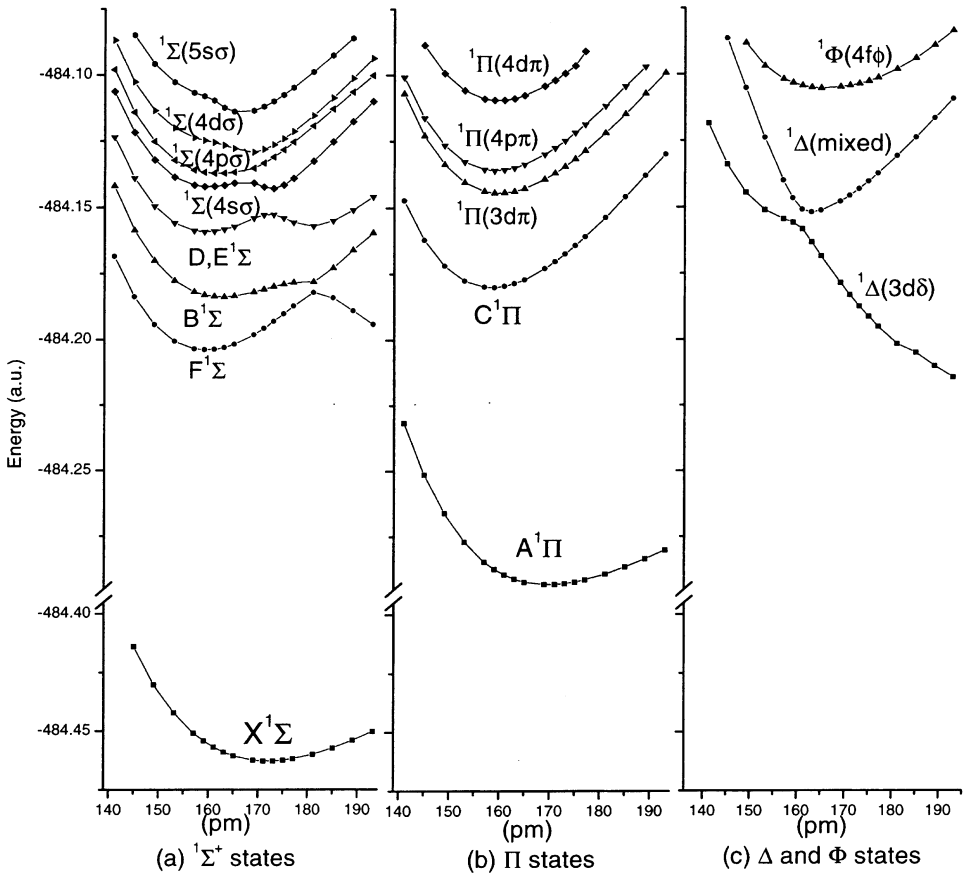

Fig. 2. The potential energy surfaces of (a) $^1\Sigma$, (b) $^1\Pi$, (c) $^1\Delta$ and $^1\Phi$ singlet states.

The properties of the $X^1\Sigma^+, A^1\Pi, F^1\Sigma^+$, and $C^1\Pi$ states are discussed first, because they not only possess relatively simple shapes of PES but also have already been well characterized by previous works [10,11]. The second part of the present discussion is about the adiabatic PES and spectroscopic constants of the $B^1\Sigma^+, D^1\Sigma^+$, and $E^1\Sigma^+$ states. The major claim in this section is the fact that the $D^1\Sigma^+$ and the $E^1\Sigma^+$ state correspond to the two stationary points on the same adiabatic PES resulting from an interaction with $\pi\pi^*(^1\Sigma^+)$ repulsive state. The last part of our discussion deals with the spectroscopic constants of new high-lying electronic states, of which any characterization has never been attempted theoretically or experimentally. The new states are four Σ, three Π, two Δ, and one Φ singlet state.

3.1. The $X^1\Sigma^+, A^1\Pi, F^1\Sigma^+$, and $C^1\Pi$ states

Irikura have determined the bond lengths of the states by parabolic interpolation between computed points. Because shapes of the $X^1\Sigma^+, A^1\Pi$, and $C^1\Pi$ states, in Fig. 2, correspond to a typical potential energy surface (PES) of a diatomic molecule, we applied the Morse function in the interpolation and fitting of the computed points between 140.0 and 193.0 pm to obtain some more reasonable results. Though we also applied the Varshni function [24], instead of the Morse function, the results are not represented here because they are virtually the same as those with the Morse function, within a few cm^{-1} for ω_e and just a few tenths of a cm^{-1} for $\chi_e\omega_e$. Because of the interstate interaction between $F^1\Sigma^+, B^1\Sigma^+$, and $\pi\pi^*(^1\Sigma^+)$

Table 1
Spectroscopic constants of the $X^1\Sigma^+$, $A^1\Pi^+$, $F^1\Sigma^+$, and $C^1\Pi$ states of $^{11}B^{35}Cl$

State		R_e (pm)	v_{00} (cm^{-1})	T_e (cm^{-1})	ω_e (cm^{-1})	$\omega_e\chi_e$ (cm^{-1})s
$X^1\Sigma^+$	Exptl.[a]	171.6	0	0	839	5.1
	Irikura[b]	171.3	0	0	864	5.6
	Present	172.0	0[c]	0	846	6.4
$A^1\Pi$	Exptl.[a]	168.9	36 754	36 751	849	11.4
	Irikura[b]	169.2	37 200	37 200	868	11.5
	Present	169.7	37 260 (−506)[d]	37 270	835	9.2
$F^1\Sigma^+$	Exptl.[a]	(160.5)[e]	55 972	–	1129	–
	Irikura[b]	159.1	56 700	56 500	1179	11.9
	Present	159.4	56 680 (−708)[d]	56 820	1128	7.3
$C^1\Pi^+$	Exptl.[a]	(160.4)[e]	61 486	–	1170	7.3
	Irikura[b]	158.1	61 900	61 700	1194	7.0
	Present	158.4	61 900 (−414)[d]	62 060	1171	6.9

[a] Experimental result by Verma. [10].
[b] Result by Irikura et al. [11].
[c] The total energy of the $X^1\Sigma^+$ state at R_e is calculated to be −484.4628329 a.u.
[d] Difference between the present calculation and experimental values.
[e] Values of R_0 instead of R_e.

states, at around 181.0 pm, as shown in Fig. 2a, the fitting of the adiabatic PES for $F^1\Sigma^+$ state to the Morse function is performed by using only the points between 140.0 and 177.0 pm. According to the t_1 amplitudes of the EOM–CCSD calculations, the F state corresponds to $\sigma \rightarrow \sigma^*$ state at internuclear distance shorter than 177.0 pm, but becomes mainly the repulsive $\pi\pi^*(^1\Sigma^+)$ state.

The equilibrium internuclear distance R_e of a state is determined by fitting five or six points around a hypothetical equilibrium bond length with third-order polynomials, and then the R_e value is fixed in the final fitting with the Morse function. In order to get the best PES for the periphery of the stationary point, no constraint on dissociation energy is imposed in the final fitting. After this, the energies of the state at equally spaced internuclear distances are generated using the fitted function. Then the vibrational levels and wavefunctions are computed by using the Fourier-grid Hamiltonian method [13]. The most abundant isotopes of B and Cl are used, which correspond to the reduced mass of 8.373167 amu. The spectroscopic constants, ω_e and $\omega_e\chi_e$, are derived by fitting the lowest six vibrational levels to the expression $G(v) = \omega_e(v + 1/2) - \omega_e\chi_e(v + 1/2)^2$.

The results of the present work are compared with the previous results in Table 1. Though the computed excitation energies (v_{00} and T_e) are larger by 414 $\sim$ 708 cm^{-1} (0.05 $\sim$ 0.09 eV) than the experimental values, mainly because the correlation of the core electrons is not included in the present work, the bond lengths (R_e) and vibrational constants (ω_e and $\omega_e\chi_e$) of this work show excellent agreement with those of the previous experimental and theoretical results [10,11]. The agreement is too good for the $F^1\Sigma^+$ and $C^1\Pi$ states.

3.2. The $B^1\Sigma^+$, $D^1\Sigma^+$, and $E^1\Sigma^+$ states

The typical shape of the PES of $B^1\Sigma^+$, $D^1\Sigma^+$, and $E^1\Sigma+$ states in Figs. 2a and 3 shows somewhat different features due to strong perturbation among themselves as well as with the F state and the repulsive state $\pi\pi^*(^1\Sigma^+)$. Because overall shape of the curves is remote from the Morse function, the calculated energies between 140 and 193 pm are interpolated by using spline functions, and the energies at equally spaced distances are generated, and then the Fourier-grid Hamiltonian method [21] is applied again. The lowest few vibrational levels and wavefunctions of the

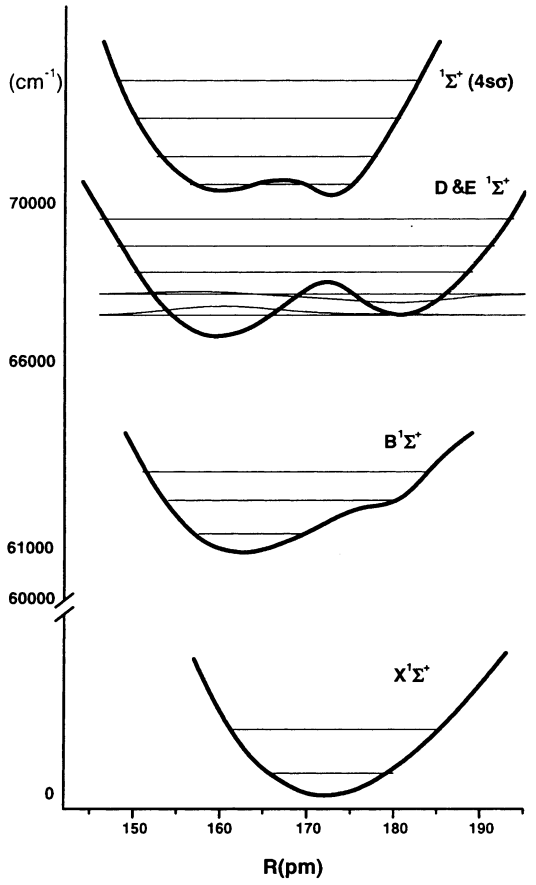

Fig. 3. The potential energy surfaces and vibration levels of the $X^1\Sigma^+$, $B^1\Sigma^+$, D, $E^1\Sigma^+$, and $^1\Sigma^+(4s\sigma)$ states.

excited B, D, and E states as well as the ground X state are depicted in Fig. 3, and the numerical values of their spectroscopic constants are presented in Table 2.

The most distinctive feature of the $B^1\Sigma^+$ state, as can be anticipated from the shape of PES in Fig. 3, is that the vibrational levels cannot be fitted into the equation, $G(v) = \omega_e(v + 1/2) - \omega_e\chi_e(v+1/2)^2$. As a result, instead of the ω_e and $\omega_e\chi_e$, we are making direct comparisons between experimentally observed $v_{v'-v''}$'s with the calculated ones in Table 2. In order to make the direct comparison more easy, the calculated values of $v_{v'-v''}$ and T_e are corrected by subtracting 846 cm^{-1}, and the corrected values are given in the lower part of Table 2. The correcting magnitude 846 cm^{-1}, which may stem from the fact that the core correlation is not included in the frozen-core approximation of this work, is so selected as to make the corrected v_{0-0} be exactly the same as the experimental value. It can be seen that the corrected values of other $v_{v'-v''}$ are also in good agreement with the corresponding experimental values. The experimental $R_e = 163.6$ pm is just 1.0 pm longer than the present $R_e = 162.6$ pm, which is also in good agreement. According to the t_1 amplitudes of the EOM-CCSD calculation, the $\sigma \rightarrow \sigma^*$ state corresponding to $3\sigma \rightarrow 3p\sigma$ is the dominant diabatic representation of the B state at the internuclear distances shorter than 173.0 pm. However due to complex interaction of F, B and diabatic state $\pi\pi^*$ at around $R_e = 177.0$ pm, the shape of the adiabatic PES of the B state takes the form as shown in Figs. 2 and 3. The B state becomes the $3\sigma \rightarrow 3s\sigma$ transition at larger R, the diabatic continuation of the $3s\sigma$ of the lower F state. According to the calculated t_1 amplitudes of our EOM-CCSD, the $3\sigma \rightarrow 3s\sigma$ transition becomes the dominant diabatic representation of the B state at $R_e = 181.0$ pm. However at R longer than 185.0 pm, the adiabatic PES of the B state become heavily mixed with $\pi\pi^*$ as well.

The adiabatic PES of the $D^1\Sigma^+$ and $E^1\Sigma^+$ state in Fig. 3 is one of the major concerns of the present work. The shape of the PES is showing that the two states correspond to the two stationary points in a single adiabatic PES with double minima. To make more quantitative discussion, spectroscopic constants are calculated and collected in Table 2. First of all, the experimentally proposed R_0's of the D and E states are within 2.0 pm from the calculated R_e's of the two stationary points in Fig. 3. The adiabatic energy separation between the two stationary points is calculated to be 474 cm^{-1}, which is slightly lower than the lowest vibrational level, $G_{v=0} = 535$ cm^{-1}. The potential barrier between the two stationary points locates at $R = 172.1$ pm with a barrier height of 1450 cm^{-1}, which is between the first and second excited vibrational levels, $G_{v=1} = 1043$ cm^{-1} and $G_{v=2} = 1609$ cm^{-1}. The calculated vibrational wavefunctions of the two states show that the first vibrational level ($v = 0$) is localized mainly at the first stationary point with little penetration into the

Table 2
Spectroscopic constants of the $B^1\Sigma^+$, $D^1\Sigma^+$, and $E^1\Sigma^+$ states of $^{11}B^{35}Cl$

State	$B^1\Sigma^+$	$D^1\Sigma^+$		$E^1\Sigma^+$
Experiment[a]				
R_e (pm)	163.6 (162.0)[b]	(161)[c]		(179)[c]
$\nu_{v'-v''}$ (cm^{-1})	60 422 (0–0)	65 862 (0–0)		
	61 293 (1–0)			66 180 (0–0)
	62 163 (2–0)	66 904 (1–0)		
		67 119 (2–1)		
Present work				
R_e (pm)	162.6	159.3		180.9
$G_{v=0}$ (cm^{-1})	464		535	
$G_{v=1}$ (cm^{-1})	1297		1043	
$G_{v=2}$ (cm^{-1})	1979		1609	
$G_{v=3}$ (cm^{-1})	2794		2278	
T_e (cm^{-1})	61 227		66 659	
	60 381[d]		65 749[e]	
$\nu_{v'-v''}$ (cm^{-1})	60 422[d] (0–0)		65 862[e] (0–0)	
	61 255[d] (1–0)		66 370[e] (1–0)	
	61 937[d] (2–0)		66 936[e] (2–0)	
			67 456[e] (4–1)	
			67 605[e] (3–0)	

[a] Experimental result by Verma. [10].
[b] Results by Irikura et al. [11].
[c] Value of R_0 instead of R_e.
[d] The corrected value. See the text for detail.
[e] The corrected value. See the text for detail.

second stationary point, while the second level ($v = 1$) is localized at the second structure with a small quantum tunneling into the first region.

The interpretation of each transition $\nu_{v'-v''}$ is tentatively suggested by the experiment [10]. In order to make a direct comparison between calculated and experimental $\nu_{v'-v''}$, the calculated numbers are subtracted by 910 cm^{-1} to make corrected values given in the lower part of Table 2. The magnitude of the correction 910 cm^{-1}, which stems from the frozen-core approximation of this work, is so selected to make the corrected ν_{0-0} to be exactly the same as the corresponding experimental value. The upper part of Table 2 illustrates the observed transition frequencies and their designations proposed by the experiment [10], while the lower part represents our corrected values and interpretations. The comparison between experimental and calculated values shows that the experimental ν_{0-0} of $E^1\Sigma^+$ and ν_{1-0} and ν_{2-1} of $D^1\Sigma^+$ correspond to the calculated ν_{1-0}, ν_{2-0}, and ν_{4-1}, respectively. The good agreement between the experimentally observed values and our calculated numbers for $\nu_{v'-v''}$ is supporting our claim that the $D^1\Sigma^+$ and $E^1\Sigma^+$ state are not two distinctive states, but just two stationary points on the PES of a state resulting from the mixture of three states, two Rydberg $3d\sigma, 3p\sigma$ and a valence state $\pi\pi^*$. We tentatively designate this state as the $D, E^1\Sigma^+$ state.

The shape of the adiabatic PES suggests that the $D, E^1\Sigma^+$ state may be interpreted as $3d\sigma$ state at shorter R, the $\pi\pi^*(^1\Sigma^+)$ state at central R, and at larger R the $3\sigma \rightarrow 3p\sigma$ transition, corresponding to the continuation of the B state. According to the calculated t_1 amplitudes of the EOM-CCSD, the $\sigma \rightarrow \sigma^*$ transitions are dominant when R is shorter than 161.0 pm and longer than 181.0 pm, but $\sigma \rightarrow \sigma^*$ and $\pi \rightarrow \pi^*$ transitions are complicatedly mixed at R between 165.0 and 177.0 pm.

3.3. New Σ, Π, Δ, and Φ singlet states

The results of the present calculations have revealed the existence of other additional new excited states, which can be understood in conjunction with the state correlation diagram in

Table 3
The equilibrium bond length R_e, adiabatic excitation energy T_e[a] and vibrational levels G_v of new high-lying excited states of $^{11}B^{35}Cl$

State	R_e (pm)	T_e (cm^{-1})	$G_{v=0}$ (cm^{-1})	$G_{v=1}$ (cm^{-1})	$G_{v=2}$ (cm^{-1})
$^1\Sigma^+(4s\sigma)$	172.6 (159.7)[b]	70 190 (70 360)[b]	499	1047	2003
$^1\Sigma^+(4p\sigma)$	161.7	71 460	458	1445	2516
$^1\Sigma^+(4d\sigma)$	168.3	73 180	676	1702	2659
$^1\Sigma^+(5s\sigma)$	166.6	76 510	684	1924	2916
$^1\Pi(3d\pi)$	159.9	69 880	559	1685	2803
$^1\Pi(4p\pi)$	159.2	71 740	574	1714	2844
$^1\Pi(4d\pi)$	159.7	77 560	578	1751	2680
$^1\Delta$(mixed)	162.9	68 210	896	2434	3872
$^1\Phi(4f\phi)$	165.6	78 440	417	1236	2066

[a] Relative to the ground state, $X^1\Sigma^+$.
[b] The first stationary point of $^1\Sigma^+(4s\sigma)$ state. See Fig. 3.

Fig. 1. In addition to the states discussed above, several additional singlet states can be discerned in Fig. 2. The four high-lying Σ states in Fig. 2a, three high-lying Π states in Fig. 2b, and two Δ and one Φ states in Fig. 2c are tentatively designated as $^1\Sigma^+(4s\sigma)$, $^1\Sigma^+(4p\sigma)$, $^1\Sigma^+(4d\sigma)$, $^1\Sigma^+(5s\sigma)$, $^1\Pi(3d\pi)$, $^1\Pi(4p\pi)$, $^1\Pi(4d\pi)$, $^1\Delta(3d\delta)$, $^1\Delta$(mixed), and $^1\Phi(4f\phi)$, respectively. The designations, $^1\Delta(3d\delta)$ and $^1\Delta$(mixed), follow Irikura's work [11]. Because there is little reason to assume any special function for their PES, we have applied the spline interpolation method as used for the $D,E\,^1\Sigma^+$ state, and the vibrational levels are computed with the Fourier-grid Hamiltonian method, as above.

The calculated equilibrium distances, adiabatic excitation energies, and the lowest three vibrational levels of the states are given in Table 3, in which the $^1\Delta(3d\delta)$ state is excluded because it seems to be purely repulsive with no stationary point. As shown in Fig. 3, the PES of the $^1\Sigma^+(4s\sigma)$ state is very similar to that of the $D,E\,^1\Sigma^+$ state, and similar discussion may be applied here. The first stationary point of the $^1\Sigma^+(4s\sigma)$ at $R = 159.7$ pm is higher by only 170 cm^{-1} than the second stationary point at $R = 172.6$ pm, and the energetic separation is even lower than the lowest vibrational level, $G_{v=0} = 499$ cm^{-1}. The barrier between the two stationary point locates at $R = 167.2$ pm, and the barrier height is calculated to be 570 cm^{-1}, which is higher than the lowest vibration level, but lower than the first excited vibration level, $G_{v=1} = 1047$ cm^{-1}. The vibration levels of the states in Table 3, except the $^1\Sigma^+(4s\sigma)$, may be fitted into the equation, $G(v) = \omega_e(v+1/2) - \omega_e\chi_e(v+1/2)^2$, to get the vibrational constants, ω_e and $\omega_e\chi_e$.

It must be noted that the upper left part of the PES of $^1\Delta(3d\delta^*)$ is parallel with the left part of the PES of $D,E\,^1\Sigma^+$ state, and they are very close energetically. If the two figures, Fig. 2a,c, are overlapped, such a relationship can be seen easily. It might be better to designate $^1\Delta(3d\delta^*)$ as $^1\Delta(\pi\pi^*)$ valence state [1], but the leading configuration of the $^1\Delta(3d\delta$ or $\pi\pi^*)$ along the internuclear distance could not be discerned clearly, and Irikura's designation is just recited here. Though we suggest the possibility that the PES of the $^1\Delta(3d\delta$ or $\pi\pi^*)$ state could be relevant to the predissociation of the $D,E\,^1\Sigma^+$ state, which was observed experimentally by Verma [9], further details about such internal conversion and/or the nonadiabatic interactions between electronic states in dynamic phenomena, however, are beyond the scope of this work, and are not explored here. Although any further discussion in detail about these new high-lying states is not attempted here, we hope the information provided here could be useful in future experimental works.

4. Conclusions

In order to characterize the PES of excited singlet states of BCl, the equation-of-motion

[1] Authors thank the referee for suggesting this interpretation.

coupled-cluster singles and doubles (EOM-CCSD) method is applied in conjunction with the (16s11p5d3f)/[9s9p5d3f], and the (18s13p5d4f)/[8s8p5d4f] basis for B and Cl, respectively. Though the excitation energies are calculated to be about $0.05 \sim 0.1$ eV higher than experimental values, mainly because the frozen-core approximation of the present work does not include the core correlation effect, the effects of the frozen-core on spectroscopic constants seem to be less than 1% of the calculated values as shown elsewhere for ground states [18] and excited states [19,20] of several simple molecules.

The PES of the $X\,^1\Sigma^+, A\,^1\Pi, F\,^1\Sigma^+$, and $C\,^1\Pi$ states around their equilibrium bond length are obtained by fitting calculated energies into the Morse function. Due to interstate perturbation between $^1\Sigma^+$ states, on the other hand, the PES of $B\,^1\Sigma^+, D\,^1\Sigma^+$, and $E\,^1\Sigma^+$ states turn out to be away from a typical shape of the Morse function, and the PESs are obtained by using spline fitting of the calculated energies. The vibrational levels on a PES are computed by using the Fourier-grid Hamiltonian method.

The spectroscopic constants of the X, F, A, B, and C electronic states in this work show an excellent agreement with the previous experimental and theoretical works. It is shown that the $D\,^1\Sigma^+$ and $E\,^1\Sigma^+$ states correspond to the two stationary points on the same adiabatic potential energy surface.

The spectroscopic constants of newly uncovered four Σ, three Π, two Δ, and one Φ states are provided, and we expect the results to be useful in future spectroscopic and dynamic studies.

Acknowledgements

This work was supported by the Korea Research Foundation under Grant No. KRF-99-041-D00232 D3001. Authors acknowledge the help of and discussions with Prof. R.J. Bartlett.

References

[1] D. Flamm, Solid State Technol. 36 (1993) 49.
[2] S.J. Pearton, W.S. Hobson, C.R. Abernathy, F. Ren, T.R. Fullowan, A. Katz, A.P. Perley, Plasma Chem. Plasma Proc. 13 (1993) 311.
[3] K.K. Baeck, R.J. Bartlett, J. Chem. Phys. 106 (1997) 4604.
[4] A.G. Maki, F.J. Lovas, R.D. Suenram, J. Mol. Spectrosc. 91 (1982) 424.
[5] J. Lebreton, L. Marsigny, J. Ferran, C. R. Acad. Sci. Paris, Ser. C. 271 (1971) 1094.
[6] Y. Endo, S. Shuji, E. Hirota, Bull. Chem. Soc. Jpn. 56 (1983) 3410.
[7] G.R. Herzberg, W. Hushley, Can. J. Res. Sect. A 19 (1941) 127.
[8] E. Miescher, Helv. Phys. Acta 8 (1935) 279.
[9] R.D. Verma, J. Mol. Spectrosc. 7 (1961) 145.
[10] R.D. Verma, J. Mol. Spectrosc. 169 (1995) 295.
[11] K.K. Irikura, R.D. Johnson III, J.W. Hudgens, J. Phys. Chem. A. 104 (2000) 3800.
[12] J.F. Stanton, R.J. Bartlett, J. Chem. Phys. 98 (1993) 7029.
[13] J.E. Del Bene, J.D. Watts, R.J. Bartlett, J. Chem. Phys. 106 (1997) 6051.
[14] Advanced Concepts in Electronic Structure Theory (ACES-II) – A product of the University of Florida, Quantum Theory Project, developed by J.F. Stanton et al. Integral packages included are VMOL (J. Almlof and P.R. Taylor); VPROPS (P. Taylor); ABACUS (T. Helgaker, H.J. Ha Jensen, P. Jorgensen, J. Olsen, P.R. Taylor).
[15] P.O. Widmark, P.A. Malmqvist, B.O. Roos, Theor. Chim. Acta 79 (1991) 419.
[16] T.H. Dunning Jr., P.J. Hay, in: H.F. Shaefer III (Ed.), Methods of Electronic Structure Theory, Plenum Press, New York, 1977, p. 1.
[17] G.D. Purvis III, R.J. Bartlett, J. Chem. Phys. 76 (1982) 1910.
[18] K.K. Baeck, R.J. Bartlett, J. Chem. Phys. 109 (1998) 1334.
[19] K.K. Baeck, J. Chem. Phys. 112 (2000) 1.
[20] K.K. Baeck, S.I. Jeon, Bull. Korean Chem. Soc. 21 (2000) 720.
[21] C.C. Marston, G.G. Balint-Kurti, J. Chem. Phys. 91 (1989) 3571.
[22] C.E. Moore, Nat. Stand. Ref. Data Ser., Nat. Bur. Stand. 35 (1971).
[23] E. Wigner, E.E. Witmer, Z. Physik 51 (1928) 859.
[24] Y.P. Varshni, R.C. Shukla, J. Chem. Phys. 40 (1964) 250.